Heliyon 8 (2022) e09726

Contents lists available at ScienceDirect

Heliyon

journal homepage: www.cell.com/heliyon

Research article

The exploration of bio-inspired copper oxide nanoparticles: synthesis, characterization and in-vitro biological investigations

Lalitha Ammadu Kolahalam [a], K.R.S. Prasad [a,**], P. Murali Krishna [b,*], N. Supraja [c], S. Shanmugan [d]

[a] Department of Chemistry, Koneru Lakshmaiah Education Foundation, Vaddeswaram, Guntur, 522502, Andhra Pradesh, India
[b] Department of Chemistry, Ramaiah Institute of Technology (Autonomous Institute, Affiliated to VTU), Bangalore, 560054, Karnataka, India
[c] Acharya N G Ranga Agricultural University, Nanotechnology Laboratory, RARS, Tirupati, 517502, Andhra Pradesh, India
[d] Research Centre for Solar Energy, Department of Physics, Koneru Lakshmaiah Education Foundation, Vaddeswaram, Guntur, 522502, Andhra Pradesh, India

GRAPHICAL ABSTRACT

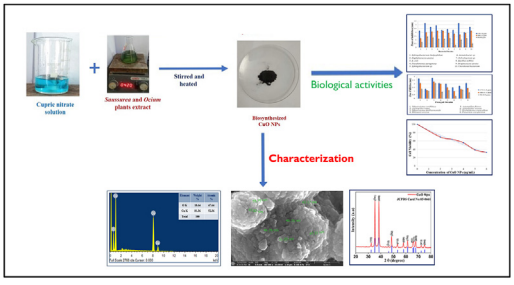

ARTICLE INFO

Keywords:
Copper oxide nanoparticles
Antibacterial
Antifungal
Cytotoxic activity
Ocimum sanctum and *Saussurea lappa* plant extracts

ABSTRACT

The paper describes the synthesis and characterization of copper oxide nanoparticles (CuO NPs) using the mixture of plant rhizome extracts *Ocimum sanctum* and *Saussurea lappa* as a reducing agent. The prepared CuO nanoparticles are characterized and confirmed their formation based on data obtained from powder X-ray diffraction spectroscopy, Fourier Transmission Infrared, Ultraviolet-Visible spectra, Field Emission Scanning Electron Microscopy images, Energy Dispersive X-ray analysis and Dynamic light scattering techniques and data reveal that the average size of CuO Nps was 103.4 nm. The result of antibacterial and antifungal activities for concentrations 50, 100, and 170 ppm indicate that NPs may exhibit appreciable activity at higher (170 ppm) concentrations. The MTT cytotoxic assay studies of Chinese Hamster Ovary (CHO) cell lines showed a Half-maximal inhibitory concentration (IC_{50}) value of 4.14 μg/mL.

1. Introduction

Advanced nanotechnology is an emerging area of science and technology because of its minimal size of nanomaterials. The unique optical, electrical, and catalytic properties of the metal-oxide nanomaterials attracted the scientific community and applied them to biomedical, catalytic, biosensors, electronics, food, photonics, and many other studies [1, 2, 3, 4, 5]. Copper oxide is one of the transition metal oxides

* Corresponding author.
** Corresponding author.
E-mail addresses: krsprasad_fed@kluniversity.in (K.R.S. Prasad), muralikp@msrit.edu (P.M. Krishna).

https://doi.org/10.1016/j.heliyon.2022.e09726
Received 4 February 2022; Received in revised form 27 March 2022; Accepted 9 June 2022

containing a narrow bandgap and their good electrochemical activity, stability in solutions, high surface area and good redox potentials [6] copper oxide nanoparticles have immense applications in various fields such as sensors, catalysis, energy storage, photonic devices, biomedical, chemical and biological sensing, light emitters, health care to decrease tumour cell viability [7, 8, 9, 10, 11, 12]. As copper has anti-fungal and anti-bacterial properties, it is used to improve the skin features of the face by utilizing copper oxide pillows [13]. In diabetic patients, copper impregnated socks are used to minimize the risk of skin pathology [14]. In recent years with the advent of nanotechnology, copper oxide nanomaterials have gained interest and applied as anti-diabetic, anti-microbial agents [15, 16, 17, 18] and also in bio medicinal research as biomaterials and optoelectronic fields [19, 20].

Over the past few decades, the synthesis of metal and metal oxide nanoparticles such as gold (Au), silver (Ag), and copper (Cu) has gained interest mainly in the biomedical field, especially in biosensing, imaging, diagnosis, and therapy [21]. Among, cheap, reactive catalysts with high yield [22], an essential element for humans [23], and also present in enzymes like superoxide dismutase, cytochrome oxidase, and tyrosinase [24] copper and/or copper oxide nanoparticles showed an interest in synthesis and investigation of their biological activities. The copper oxide nanoparticles are abundantly used as anticancer, antimicrobial, and antioxidant agents due to the interaction of nanoparticles with the cellular components, which leads to the participation of several reactions and functions in the biological system [25, 26, 27, 28, 29]. To overcome the limitations in chemical, physical, and biological methods [30, 31, 32, 33], an inexpensive, eco-friendly, non-toxic green synthesis method using plant extracts as a reducing agent and fueling agent is adopted during the synthesis of nanomaterials [34]. As the plant extract contains components such as tannins, flavonoids, and terpenoids which act as stabilizers during the synthesis of nanoparticles [35, 36, 37] leading to the minimal use of chemicals.

The *Ocimum sanctum* plant belongs to the Lamiaceae family, commonly known as Tulsi, the Queen of Herbs, India's legendary 'Incomparable'. It has a significant role in the Hindu religion with spiritual holiness, which links the plant with the figure of the goddess and is known from the traditional Ayurvedic epoch. In Ayurveda, its extracts are used majorly for colds, headaches, inflammations and gastrointestinal disorders [38]. *Saussurea lappa* plant is related to the Asteraceae family and is popularly known as Costus, Kushta. Usually, this plant grows in higher altitudes, Himalayan ranges of around 9000 feet, Western Ghats, Korea, Japan and China [39]. Since ancient times, this herb has been used as an anti-asthmatic, antidysentery, anti-inflammatory, and anti-ulcerative [40, 41].

From the literature survey, it is observed that the *Ocimum* species used for the synthesis of silver [42, 43], gold [44], platinum [45], copper [46] and zinc [47] oxide nanomaterials. *Saussurea lappa* plant rhizome extract was utilized in the synthesis of silver [48], magnesium [49] selenium [50], and zinc oxide [51] nanoparticles but no literature on the synthesis of copper oxide (CuO) nanoparticles. In addition, best of our knowledge, there is no literature available on the synthesis of copper oxide (CuO) nanoparticles using a mixture of both *Ocimum sanctum* and *Saussurea lappa* plant extracts. In the view of the above and continuity of our work on the synthesis of nanomaterials using *Saussurea lappa* plant extract [51], and also medicinally important copper oxide nanoparticles [52] herein reporting the synthesis of copper nanoparticles and their anti-bacterial, antifungal and cytotoxic studies.

2. Materials and methods

2.1. Materials

Copper-nitrate (98% AR) is obtained from Merck, Pvt. Ltd, India. The Chinese Hamster Ovary (CHO) cell lines were obtained from the National Centre for Cell Sciences in Pune, India. The electronic spectrum of the material was measured between 200 and 800 nm with the Spectra 450 SHIMADZU UV-Visible Spectrophotometer. The size, distribution and zeta potential of the nanoparticles were measured using the Dynamic light scattering (DLS) technique (Nanopartica, HORIBA, SZ-100). The Attenuated Total Reflectance Fourier Transform Infrared (ATR-FTIR) spectrum was recorded in the range of 500-4000 cm^{-1} with the KBr pellet method. The crystallinity of the nanoparticles was obtained by the Rigaku Miniflex 600, Japan X-Ray Diffraction (XRD) analysis. The shape, size, and external morphology of the NPs were explained with F-50 of Field Emission Scanning Electron Microscopy (FESEM) and for Elemental analysis done by EDX of the model Energy Dispersive X-ray (EDX) spectroscopy of model FEI-Quanta FEG 200F at IIT- Chennai, Tamil Nadu. The DSC/TGA (Differential Scanning

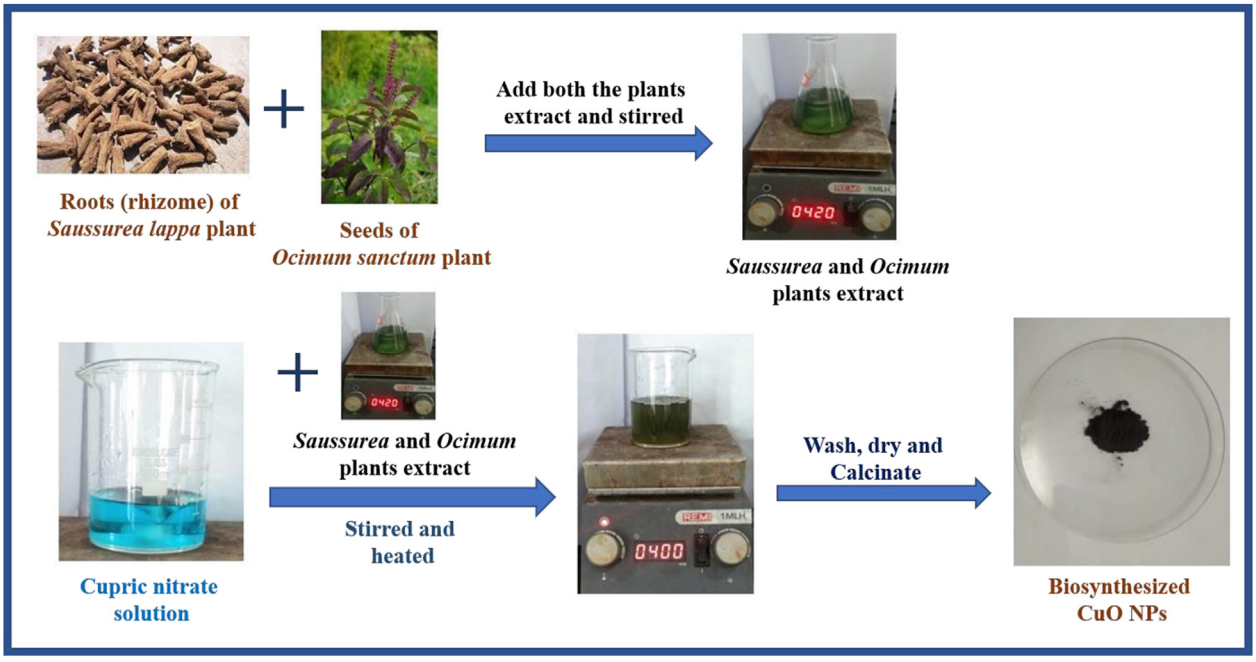

Figure 1. Biosynthesis of CuO NPs from *Ocimum sanctum* and *Saussurea lappa* plant extract.

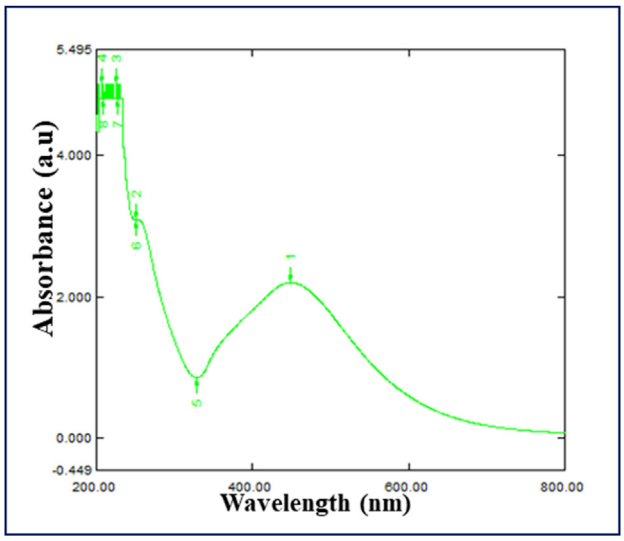

Figure 2. The UV-Visible spectrum of biosynthesized CuO nanoparticles.

Calorimetry/Thermal Gravimetric Analysis) studies were studied using a NETZSCH STA 449F3 thermogravimetric instrument at the Ramaiah Institute of Technology, Bangalore.

2.2. Extraction of the plants

The seed extract of *Ocimum sanctum* and root (rhizome) extract of the *Saussurea lappa* was used to prepare the Copper oxide nanomaterials. The extract was obtained using the following steps. Fresh seeds of *Ocimum sanctum* were collected in Vijayawada, Andhra Pradesh, India. The collected seeds were thoroughly washed with double distilled water, and dry it under the shade. The dried seeds were crushed and powdered. To a 100 ml of distilled water added 1 gm of seed powder, then boiled at 70 °C for about 30 min, cooled, filtered, and store at 4 °C in the refrigerator for further use. The root extract of the *Saussurea-lappa* plant was prepared following the procedure described by the same group [51].

2.3. Preparation of copper oxide nanoparticles from plant extract

Using a mixture of *Ocimum sanctum* and *Saussurea lappa* plant extract as a reducing agent and fuel, CuO nanoparticles were synthesized by the Co-precipitation procedure (Figure 1). To a stirred mixture of both the plant extracts (50 ml in 1:1v/v) added an aqueous solution of copper nitrate solution (0.1M) and continued stirring for 15 min then another 20 min at 60 °C. The stirring may be continued until the solution colour changed from light to dark colour along with precipitation formation. Then, centrifuged and washed with distilled several times, and dried, ground with mortar and pestle. Finally, calcinate the powder at 700 °C for 4 h.

2.4. Biological studies

2.4.1. Isolation of test organisms and antimicrobial activity

Eight varieties of fungi (*Meyerozyma caribbica* and *guilliermondii, Aspergillus niger, flavus* and *oryza, Rhizopus oryzae, Trichoderma asperellum* and *Fusarium oxysporium)* and ten varieties of bacterial (*Staphylococcus aureus*, *Sphingobacterium thalpophilum, E. coli, P. aeruginosa, Sphingobacterium sp, Acinetobacter sp, Ochrobactrum sp, B. subtilis, S. aureus* and *Uncultured bacterium* species were segregated from the drinking water

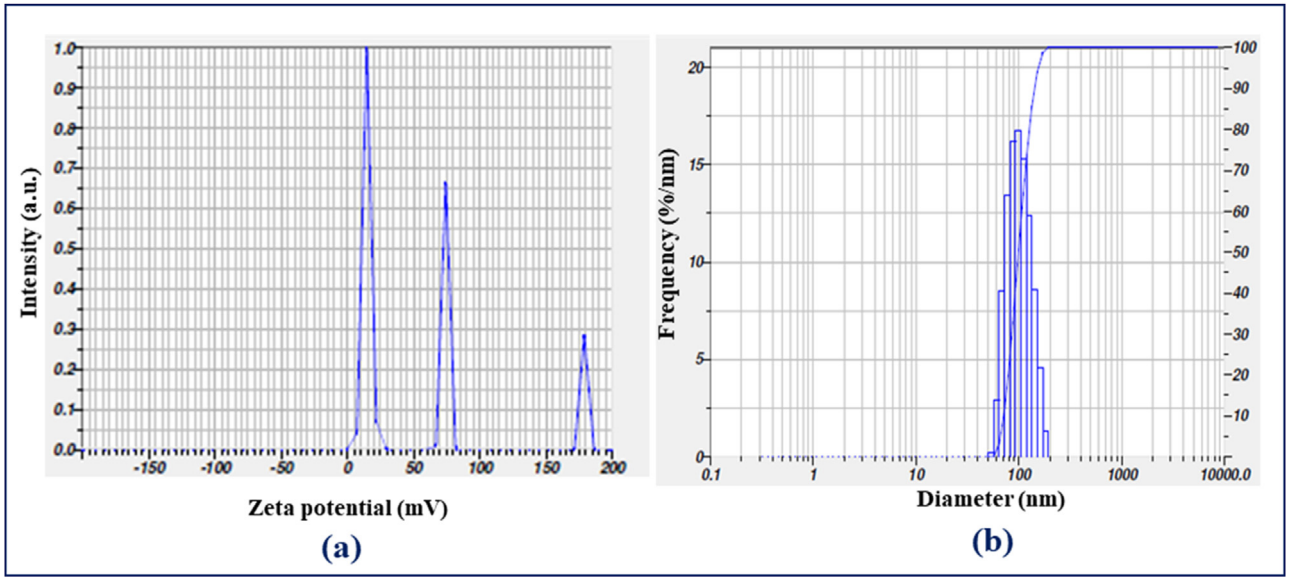

Figure 3. Histogram of biosynthesized CuO NPs using (a) Zeta potential and (b) Dynamic light scattering.

Table 1. Dynamic light scattering and Zeta potential data of synthesized CuO nanoparticles.

Particle Size					Zeta Potential		
Peak No	S P area ratio	Mean (nm)	SD (nm)	Mode (nm)	Peak No	Zeta Potential (mV)	Electrophoretic Mobility mean (cm^2/Vs)
1	1.00	103.4	27.4	98.5	1	14.9	0.000116
2	-	-	-	-	2	74.3	0.000577
3	-	-	-	-	3	178.8	0.001389
Total	1.00	103.4	27.4	98.5		63.2	0.000491

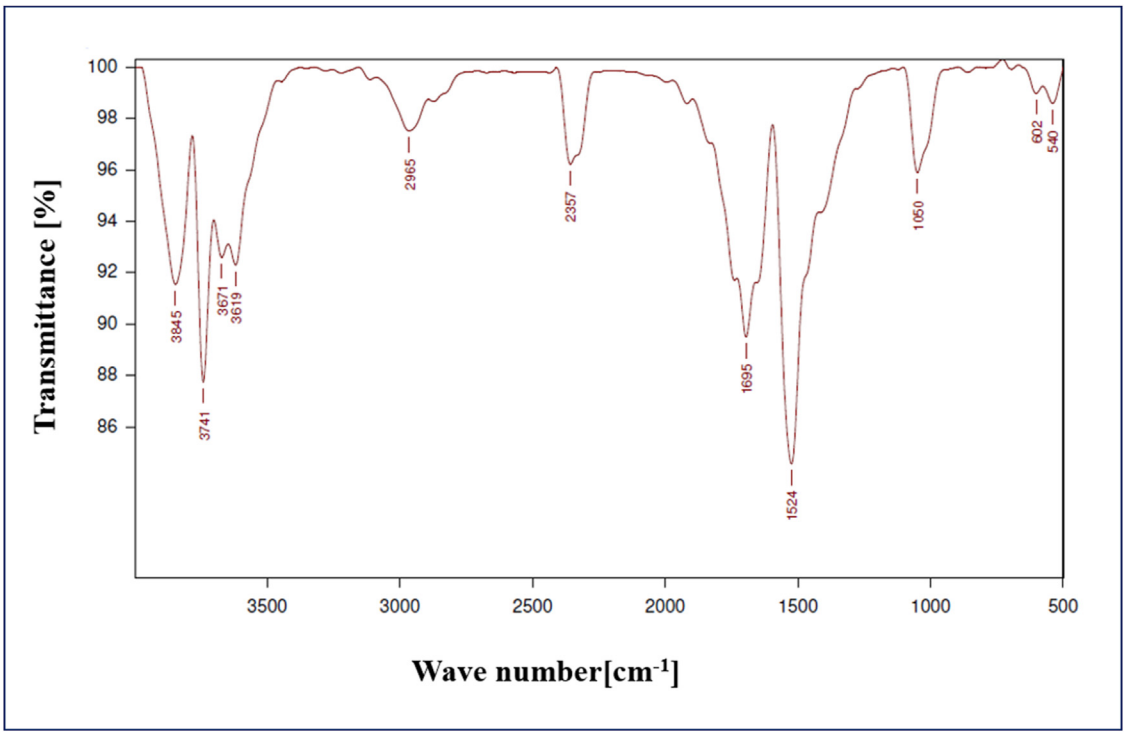

Figure 4. FT-IR spectrum of biosynthesized CuO nanoparticles.

supply of the PVC pipeline in Tirupati town, Chittoor district, Andhra Pradesh, India. Using potato dextrose agar medium and nutrient agar medium the fungal and bacterial species respectively were isolated through the serial dilution pour plate technique. Then they are maintained for further investigations in potato dextrose agar slants and nutrient agar slants for fungal and bacterial species growth. The fungal and bacterial strains were grown in the respective medium and were collected (10 days for bacterial and 2 days for fungal strains) and incubated at 37 °C. The antimicrobial activity of the biosynthesized CuO-NPs was performed for three different concentrations of (50, 100, and 170 ppm) using the disk diffusion method. Then, the size of the zone of inhibition was calculated by measuring the diameter of the zone in millimetres.

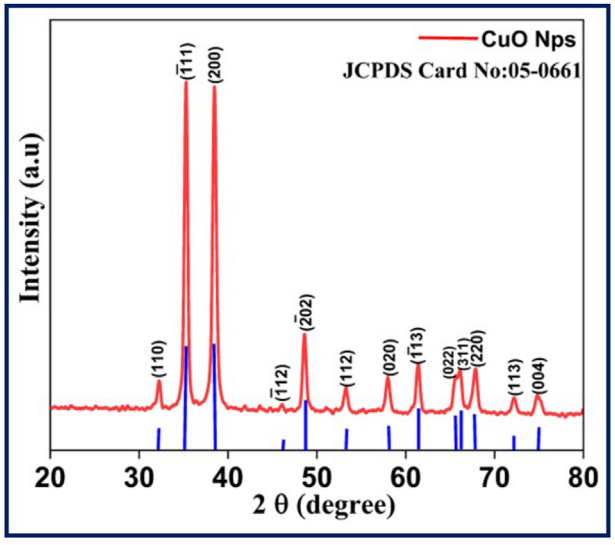

Figure 5. X-ray diffractogram of CuO nanoparticles obtained using *Ocimum sanctum* and *Saussurea lappa* plant extract.

2.4.2. Cytotoxicity effect of CuO nanoparticles

The cytotoxic investigations of biosynthesized CuO nanoparticles on Chinese Hamster Ovary (CHO) cell line studies using 3-(4,5-Dimethylthiazol-2-yl)-2,5-dipm8 phenyltetrazolium bromide) (MTT) analysis method [53]. In a humidified incubator, cells were grown at 37 °C with 11% Fetal Bovine Serum (FBS) under 5% CO_2/95% air in DMEM. In 96 tissue culture plates, the CHO cells were seeded at the quantity of 2×10^5 cells per well. The CHO cells were treated with biosynthesized CuO NPs for 24 h in a humidified CO_2 incubator. These cells were then treated with 20μL of 50 mg/mL MTT and incubated for 4 h in a humidified atmosphere [54]. 200 μL of DMSO was added, and the wells were mixed to dissolve MTT formazan crystals. In a control assay, cells were developed in a similar medium without the biosynthesized CuO NPs. Immediately after the violet colour appeared; the absorbance at 570 nm was measured.

In a control, the formazan produced in the cells was treated as 100% viable. Depending on the volume of MTT converted into insoluble formazan salts, the relative cell viability is estimated. Different concentrations of nanoparticles were tested three times independently on the CHO cell lines, and the mean ± SEM was determined and expressed as a percentage of the ratio of cell viability to concentration (μM). The cell viability percentage was calculated using Eq. (1). The cytotoxicity of CuO NPs at concentrations 2, 3, 4, 5 and 6 μg/mL was tested on the CHO cell lines. The IC_{50} value was calculated using the logarithmic transformation of the CuO concentration and nonlinear regression sigmoidal dose-response analysis.

$$Cell\ Viability(\%) = \frac{Mean\ OD\ of\ CuO\ NPs}{OD\ of\ control} \times 100 \quad (1)$$

2.5. Statistical analysis

Data were obtained through replicate experiments and analyzed using SPSS version 16.0. Statistical parameters i.e. the mean ± SD and the corresponding significant differences between means were extracted using a one-way ANOVA (CRD) followed by Duncan's multiple range test (DMRT) ($P < 0.05$).

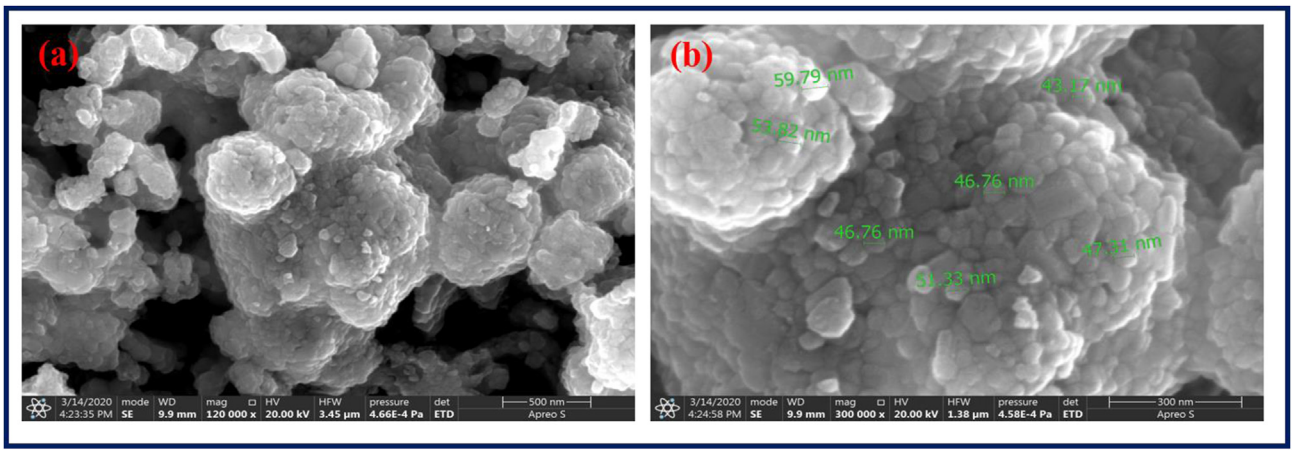

Figure 6. FESEM images of biosynthesized CuO nanoparticles under (a) 500 nm and (b) 300 nm.

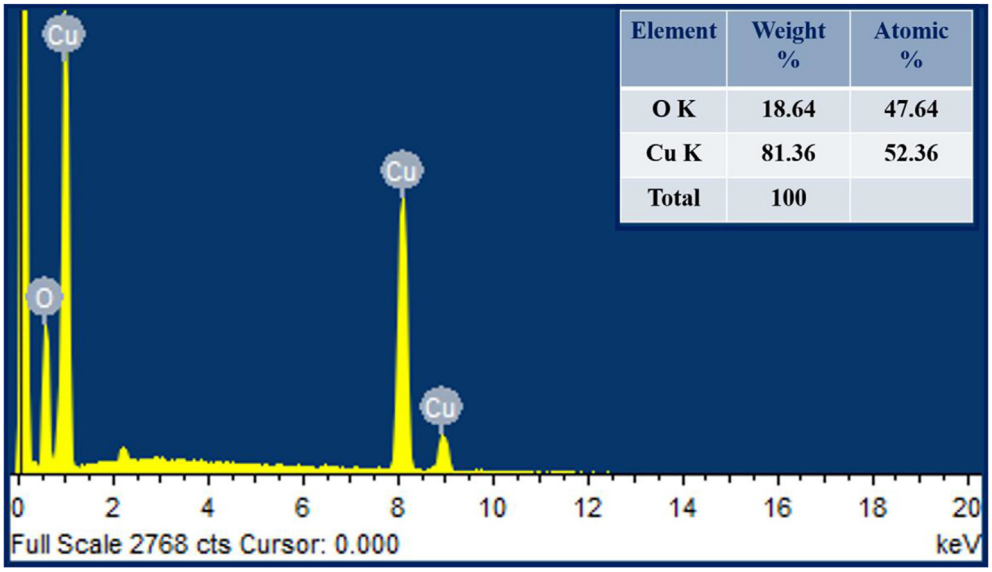

Element	Weight %	Atomic %
O K	18.64	47.64
Cu K	81.36	52.36
Total	100	

Figure 7. EDX graph and elemental analysis of synthesized CuO nanoparticles.

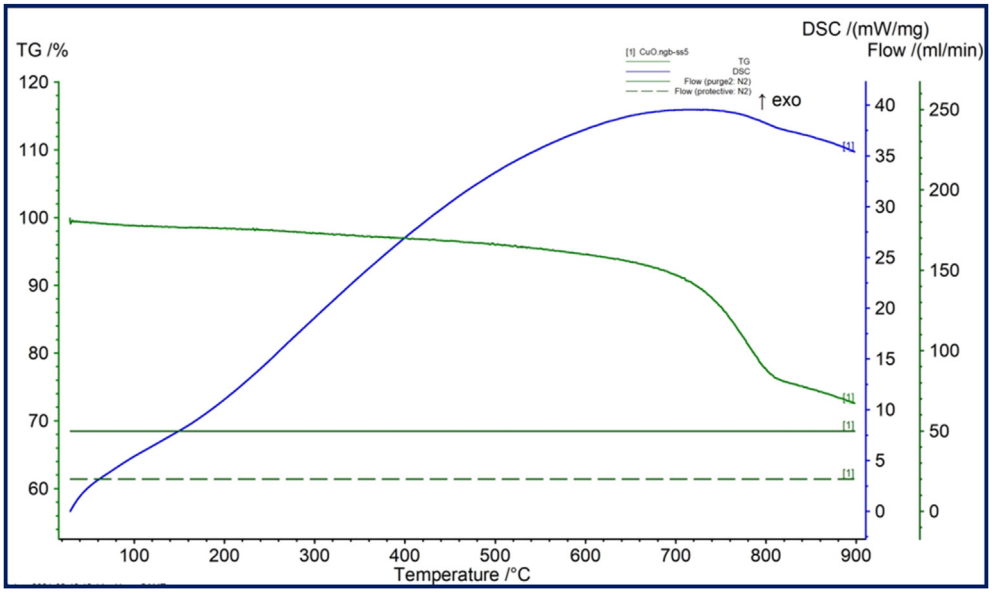

Figure 8. TGA and DSC plot of biosynthesized CuO nanoparticles using *Ocimum sanctum* and *Saussurea lappa* plant extracts.

Table 2. In-vitro antibacterial studies of synthesized CuO nanoparticles.

S No	Bacteria	Copper oxide Nanoparticles Zone of inhibition (mm)		
		170 ± 1.4 ppm	100 ± 1.1 ppm	50 ± 0.9 ppm
Gram-negative				
1	*Sphingobacterium thalpophilum*	2.2 ± 0.04^{bc}	1.2 ± 0.02^{d}	0.7 ± 0.05^{cd}
2	*Staphylococcus aureus*	3.2 ± 0.03^{a}	2.0 ± 0.05^{a}	1.4 ± 0.06^{a}
3	*E. coli*	2.7 ± 0.05^{a}	2.1 ± 0.04^{abc}	1.3 ± 0.07^{c}
4	*Pseudomonas aeruginosa*	2.9 ± 0.08^{bc}	2.2 ± 0.08^{ab}	1.1 ± 0.05^{cd}
5	*Sphingobacterium sp*	2.3 ± 0.06^{a}	2.2 ± 0.03^{a}	1.1 ± 0.16^{a}
6	*Acinetobacter sp*	2.4 ± 0.04^{b}	1.9 ± 0.04^{d}	1.2 ± 0.06^{b}
7	*Ochrobactrum sp*	2.3 ± 0.18^{de}	1.8 ± 0.01^{d}	0.3 ± 0.08^{d}
Gram-positive				
8	*Bacillus subtilis*	3.2 ± 0.14^{a}	1.7 ± 0.07^{d}	1.0 ± 0.04^{b}
9	*Streptococcus aureus*	2.0 ± 0.02^{d}	1.9 ± 0.06^{bc}	1.2 ± 0.07^{cd}
10	*Uncultured bacterium*	2.7 ± 0.17^{d}	2.2 ± 0.06^{abc}	0.5 ± 0.09^{d}
Completely Randomized Design CRD ($P \leq 0.05$)		0.245	0.200	0.139

The data presented is ±SE of three measurements and Data followed by the same letter are not significantly different at $P \leq 0.05$, whereas those followed by different letters are significantly different at $P \leq 0.05$.

3. Results and discussion

3.1. Preparation and characterization of CuO-NPs

The prepared copper oxide nanoparticles are stable at room temperature and red in colour. In the production of the copper oxide nanoparticles from the plant extract, the following reaction path Eq. (2) may occur.

$$Cu^{+2} + 2\,e^{-} \rightarrow Cu^{0} + \text{Air } (O_2) \rightarrow CuO \quad (2)$$

The formed NPs were characterized by spectroscopic methods.

3.1.1. Analysis of UV-Visible spectrum analysis

The UV-Vis spectrum of the synthesized nanoparticles was recorded in the range of 200–800 nm at various time intervals using Spectra 450, SHIMADZU spectrophotometer to monitor the evolution and stability of the synthesized CuO NPs. In Figure 2, two absorption peaks were noticed at about 270 nm and 500 nm for biosynthesized CuO nanoparticles from both plant extracts from *Ocimum sanctum* and *Saussurea lappa*. The absorption peak at 270 nm is due to CuO nanoparticles [55]. The other

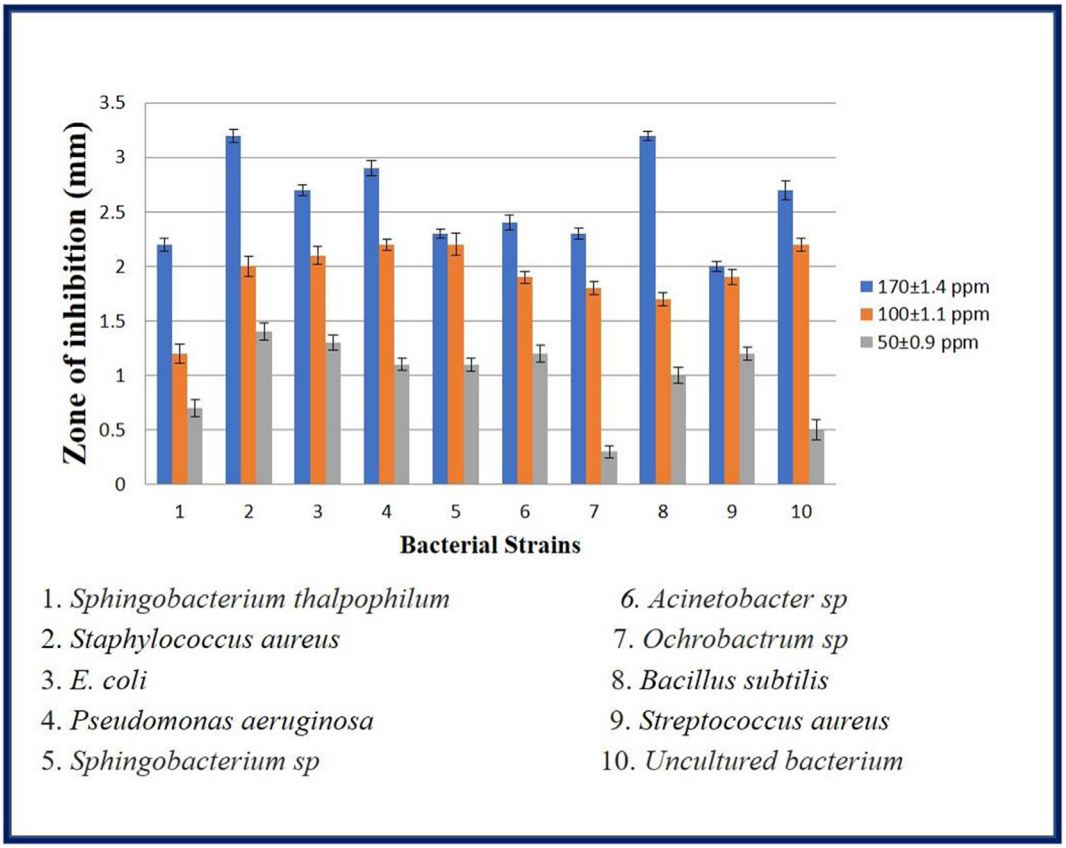

Figure 9. Bar diagram of in-vitro antibacterial studies of biosynthesized CuO nanoparticles using *Ocimum sanctum* and *Saussurea lappa* plant extracts.

Table 3. In-vitro antifungal studies of synthesized CuO nanoparticles.

S No	Fungi	Copper oxide Nanoparticles Zone of inhibition (mm)		
		170 ± 1.4 ppm	100 ± 1.1 ppm	50 ± 0.9 ppm
1	*Meyerozyma caribbica*	2.7 ± 0.12^{b}	2.1 ± 0.08^{cd}	1.3 ± 0.02^{ab}
2	*Aspergillus niger*	1.3 ± 0.14^{c}	1.1 ± 0.22^{c}	1.0 ± 0.05^{a}
3	*Meyerozyma guilliermondii*	2.8 ± 0.05^{b}	2.3 ± 0.14^{d}	2.1 ± 0.07^{a}
4	*Rhizopus oryzae*	2.1 ± 0.08^{a}	2.0 ± 0.02^{ab}	0.9 ± 0.08^{c}
5	*Aspergillus flavus*	2.0 ± 0.06^{a}	1.5 ± 0.08^{ab}	1.1 ± 0.06^{a}
6	*Aspergillus oryzae*	1.5 ± 0.04^{c}	1.0 ± 0.06^{c}	0.3 ± 0.04^{a}
7	*Trichoderma asperellum*	1.7 ± 0.08^{a}	1.3 ± 0.05^{a}	1.2 ± 0.12^{b}
8	*Fusarium oxysporium*	2.1 ± 0.02^{a}	1.4 ± 0.04^{d}	0.8 ± 0.14^{c}
Completely Randomized Design C.R.D ($P < 0.05$)		0.260	0.210	0.180

The data presented is ±SE of three measurements and Data followed by the same letter are not significantly different at $P \leq 0.05$, whereas those followed by different letters are significantly different at $P \leq 0.05$.

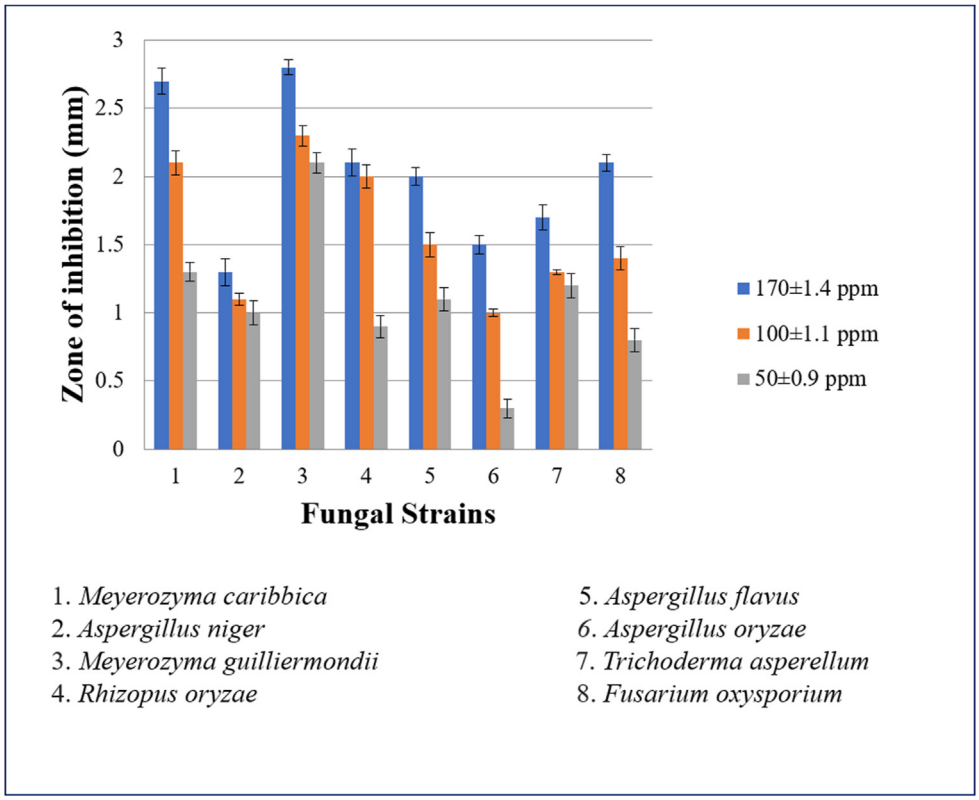

Figure 10. Bar diagram of in-vitro antifungal studies of biosynthesized CuO nanoparticles using *Ocimum sanctum* and *Saussurea lappa* plant extracts.

broad peak of 500 nm was due to the flavonoids, phenolic compounds, and sesquiterpene present in the plant extract, which caused the peak to be redshifted.

3.1.2. Dynamic light scattering analysis

Dynamic light scattering is an advantageous technique for determining the particle size, and the surface charge of biosynthesized nanoparticles can be determined using zeta possible. The formed CuO NPs were well distributed in terms of volume and intensity. The Nanopartica SZ-100 instrument was used to determine the particle size and zeta potential. Zeta potential spectra were recorded between the zeta potential (mV) on X-axis and intensity (a.u.) on Y-axis and particle size distribution spectrum was lotted between diameter (nm) on X-axis and frequency (%/nm) on Y-axis, and their results are shown in Figure 3(a and b). The stability of the nanoparticles is directly proportional to the magnitude of the charge on them. Here from Table 1, the biosynthesized CuO NPs have a zeta potential of 63.2 mV with a particle size of 103.4 nm, showing excellent stability. Zeta potential with a more positive or negative charge indicates excellent physical colloidal stability [56] and this is due to electrostatic repulsions between particles. The lower magnitude of Zeta potential is due to the accumulation of particles.

3.1.3. FT-IR studies

Figure 4 illustrates the FT-IR spectrum of copper oxide nanoparticles in the range of 4000-500 cm^{-1}. 3845, 3741, and 3671 cm^{-1} peaks correspond to O–H stretching of the free –OH group. 3619 cm^{-1} peak attributes to the C–H bond stretching vibrations of alkynes. The peak of 2965 cm^{-1} is attributed to the N–H bond stretching of amine salt. 2357 cm^{-1} peak attributes to the C≡C stretching vibrations of alkynes. 1695

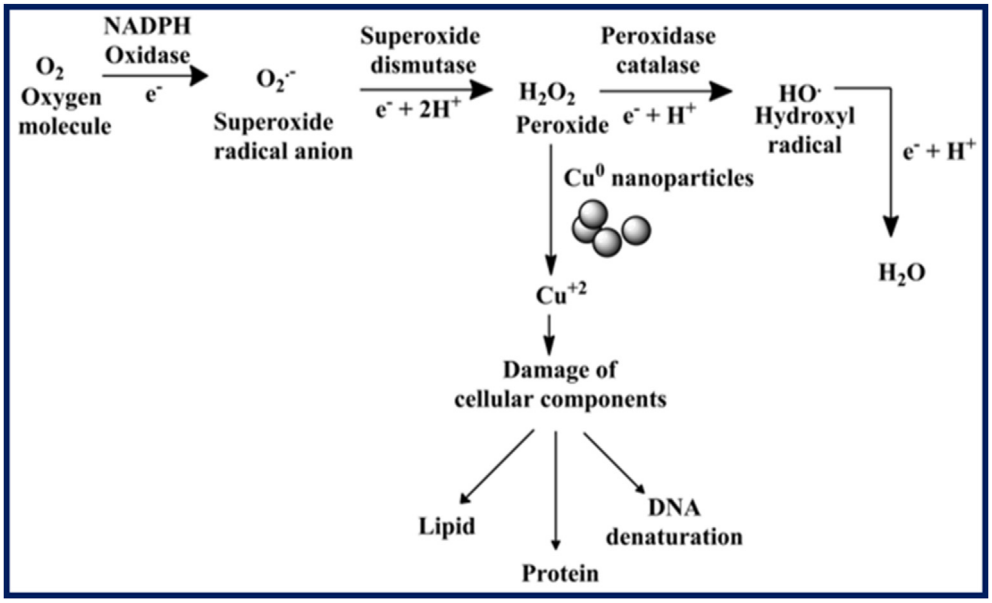

Figure 11. Schematic representation of ROS generation by CuO Nanoparticles.

cm^{-1} peak attributes to the C=O bond stretching vibrations of carboxylic acid. 1524 cm^{-1} and 1050 cm^{-1} correspond to the amine group. In that 1524 cm^{-1} corresponds to the N–H bond bending and 1050 cm^{-1} is related to the C–N bond stretching of amines. 602 cm^{-1} peaks were for C–O bending vibrations, and 540 cm^{-1} peaks were relevant to Cu–O vibrations [57].

3.1.4. XRD studies

The powder XRD patterns of the CuO Nps from the *Ocimum sanctum* and *Saussurea lappa* plant extract was shown in Figure 5. Here the formed $2\theta = 32.39^0$, 35.40^0, 38.50^0, 46.19^0, 48.67^0, 53.46^0, 58.16^0, 61.48^0, 65.66^0, 66.06^0, 67.97^0, 72.17^0, 75.10^0 peaks were clearly observed which can be set to miller indices planes of (110), $(\overline{1}11)$, (200), $(\overline{1}12)$, $(\overline{2}02)$, (112), (020), $(\overline{1}13)$, (022), (311), (220), (113), (004). These peaks were almost in good coincidence with JCPDS Postcard No.05-0661 and therefore confirmed the formation of the typical monoclinic structure of CuO nanoparticles [27, 58]. The average size of the synthesized CuO nanoparticles was around 38±1 nm calculated from Debye-Scherrer formulae [59, 60].

3.1.5. Morphological studies of copper oxide nanoparticles

The FESEM images were acquired at different magnifications to investigate the morphological studies of biosynthesized CuO NPs. From the SEM images of the CuO NPs, some of them are well-dispersed rough round, and cuboidal, closed packed nanoparticles with a higher tendency to agglomerate were observed. In them, the larger nanoparticles were surrounded by smaller nanoparticles.

In Figure 6 the copper oxide nanoparticles range in size from 40 to 60 nm. Finally, the size of the CuO Nps from FESEM results was almost in closely related to XRD studies. Figure 7 shows the EDX analysis of bio-synthesized CuO NPs calcined at 700 °C. Strong copper (Cu) signals and oxygen elements in CuO nanoparticles were observed, and the data revealed that the nanoparticles were almost stoichiometric. From the EDX analysis, the calculated weight percentage of copper is 81.36 %, and

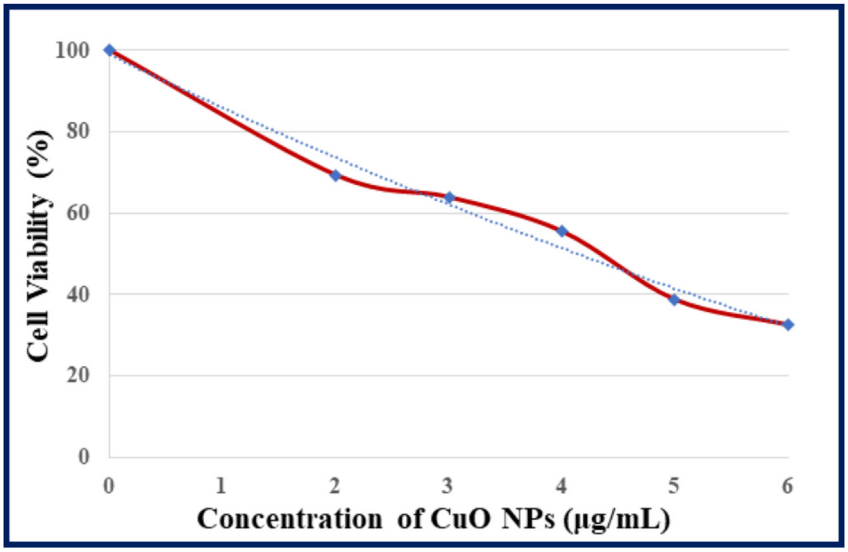

Figure 12. Graphical representation of the cytotoxic effect of biosynthesized CuO nanoparticles on CHO cell lines at different concentrations.

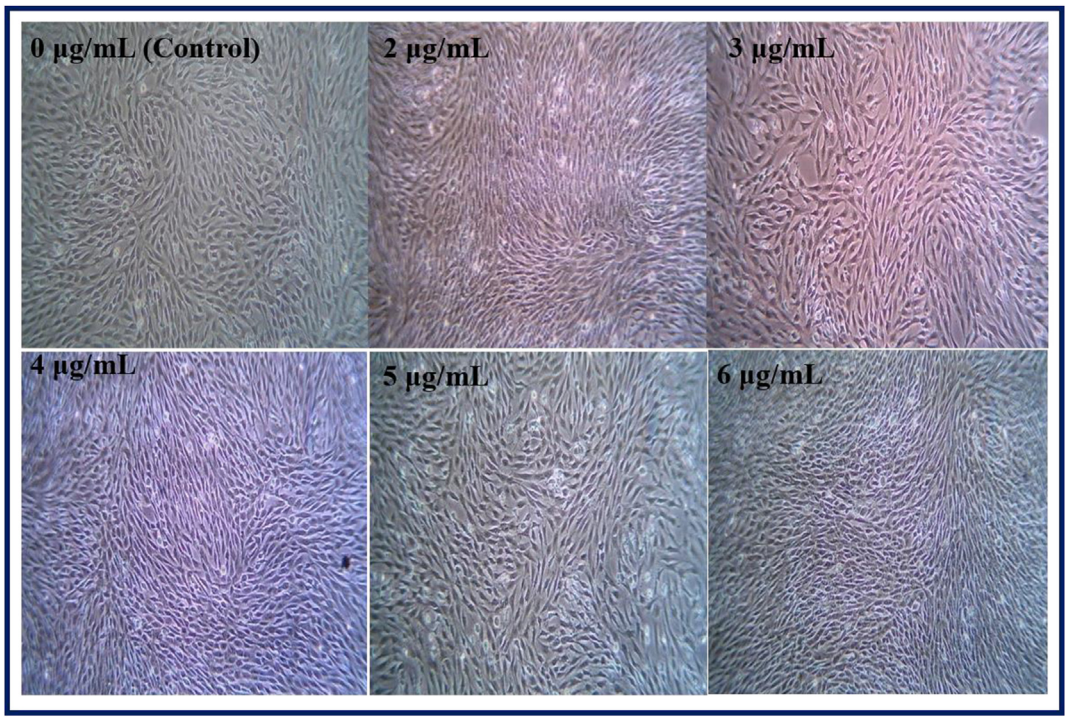

Figure 13. Cytotoxic effect of biosynthesized CuO nanoparticles on CHO cell lines at different concentrations.

oxygen is 18.64 %, and it indicated the Cu-rich environment in the lattice of biosynthesized CuO nanoparticles.

3.1.6. Thermogravimetric analysis

The thermal stability of the CuO NPs was studied by recording the thermogravimetric analysis and the Differential Scanning Calorimetry (TGA-DSC) technique from room temperature to 900 °C with a heating intensity of 10 °C/min. The TG curve of CuO is depicted in Figure 8. About 22.5% of the weight loss occurred in RT-800 °C due to the decomposition of organic matter of the plant extract of the prepared nanoparticles [61]. Then, there is no significant weight loss in the sample from 800 °C indicating the thermal stability of CuO nanoparticles. The isothermal nature of the NPs was been studied using Differential Scanning Calorimetry over the RT-900 °C temperature range. The DSC plot of the NPs (Figure 8) shows a median exothermic peak at 700 °C.

3.2. Biological studies

3.2.1. Antimicrobial action

Using disk diffusion analysis, the three different concentrations (50, 100, and 170 ppm) of biosynthesized CuO nanoparticles were taken to study the antimicrobial activity. The gram-positive microbial strains of *Bacillus subtilis, Streptococcus aureus, and* gram-negative microbial strains of *S. aureus, E. coli, Pseudomonas aeruginosa*, *Sphingobacterium species, Acinetobacter species, Ochrobactrum species* and fungal strains of *Meyerozyma species, Aspergillus species*, *Rhizopus, Trichoderma, Fusarium species* were tested for antimicrobial activity of synthesized CuO nanoparticles. The representative data of the antibacterial activities are shown in Table 2 and Figure 9. The results indicate that a higher concentration of (170 ppm) CuO NPs showed a significant antimicrobial activity than the remaining (50 and 100 ppm) concentrations [62, 63, 64]. The NPs deliver a metal ion that diffuses through the cell membrane by passive transport or interact with the bacterial membrane receptor.

The antifungal activity for the fungal strains *Meyerozyma guilliermondii* and *Meyerozyma caribbica* at concentrations of 170, 100 and 50 ppm CuO Nps was investigated and data are shown in Table 3 and Figure 10. Among, 170 ppm showed more significant antifungal activity than the remaining concentrations (100 and 50 ppm). As the concentration increases the activity also increases. The biological activity of the CuO NPs can be due to the release of reactive oxygen species (ROS) and leads to irreversible degradation of DNA. This leads to a modification of some cell components, inactivating the enzymes essential for ATP production and eventually inhibiting their regular functions [65].

In detail, the cell wall structure of gram-negative and positive bacteria is different. In general, the gram-positive bacterial cell wall consists of a thick layer of peptidoglycans than gram-negative bacteria. In many studies, it is clear that the gram-positive bacteria are more resistant to the mechanism of action of the nanoparticles than the gram-negative bacteria due to this thick layer of peptidoglycans [66, 67]. In addition, gram-negative bacteria have an outer membrane of lipopolysaccharide. As a result, both bacterial cell walls possess a negative charge and are used to influence the interaction between bacterial cell walls and ions or particles of nanoparticles. Thus, the positively charged nanoparticles can easily interact with the negatively charged cell walls due to the electrostatic attractions of opposite charges.

Nanoparticles enter the cells of microbes by directly utilizing processes such as endocytosis, phagocytosis, and macropinocytosis and also other mechanisms including hole formation, microinjection, passive diffusion and electroporation [68]. In particular, the positively charged nanoparticles change the function of the electron transport chain in the bacteria [69] since the negative charge of the bacterial cell walls attracts the positive charge of the nanoparticles. Finally, it generates reactive oxygen species (ROS) in the cell wall of bacteria which causes oxidative stress in it and finally causes the cell lysis of the bacteria (Figure 11).

3.2.2. Cytotoxic effect of CuO nanoparticles on Chinese Hamster Ovary (CHO) cell lines

Chinese hamster ovary (CHO) cell lines were used to study the in-vitro cytotoxic effect of biosynthesized CuO NPs. Different concentrations like 2, 3, 4, 5 and 6 µg/mL of CuO NPs were taken for the dosage effect. In a control experiment (0 µg/mL), the CHO cells were grown in the media without the CuO nanoparticles and absorbance was recorded at 570 nm. Independent experiments were performed and calculated the ±standard error of the mean was calculated. From the results, a graph

plotted the per cent of cell viability Vs concentration (μM). From Figure 12 and Figure 13 the effect of nanoparticle dosage at various concentrations can be observed. Here on increasing the nanoparticle concentration, the per cent of cell viability decreased and the calculated IC_{50} value is 4.14 μg/mL.

4. Conclusion

The present work addresses the biosynthesis of CuO nanoparticles from *Ocimum sanctum* and *Saussurea lappa* plant extracts which presents a simple, inexpensive, non-toxic, less chemical-use, and environmentally friendly process. From XRD results, it was observed that the CuO nanoparticles were monoclinic. The evolution of CuO NPs was confirmed by UV- Vis, XRD, DLS, FTIR and FESEM analysis. From the IR spectrum, peaks at 540 cm^{-1} were assigned to Cu–O vibrations. The size of the CuO particles is in good agreement with the results from FESEM and XRD studies. The higher concentration of 170 ppm CuO NPs showed significant antibacterial, and antifungal activity on several strains of bacteria and fungi. These nanoparticles showed significant cytotoxic activity at 6 μg/mL on Chinese Hamster Ovary (CHO) cell lines with an IC_{50} value of 4.14 μg/mL. The results obtained by the green synthesis of CuO NPs include the potential biological activities. Therefore, green synthesized CuO NPs could potentially show application in the biomedical field.

Declarations

Author contribution statement

Lalitha Ammadu Kolahalam: Conceived and designed the experiments; Performed the experiments; Analyzed and interpreted the data; Contributed reagents, materials, analysis tools or data; Wrote the paper.

K. R. S. Prasad: Conceived and designed the experiments; Analyzed and interpreted the data; Contributed reagents, materials, analysis tools or data; Wrote the paper.

P. Murali Krishna: Analyzed and interpreted the data; Contributed reagents, materials, analysis tools or data; Wrote the paper.

N. Supraja: Performed the experiments; Analyzed and interpreted the data; Contributed reagents, materials, analysis tools or data.

S. Shanmugan: Analyzed and interpreted the data; Wrote the paper.

Funding statement

This work was supported by the Management and Trust of Koneru Lakshmaiah Education Foundation Vaddeswaram, Andhra Pradesh, India.

Data availability statement

Data included in article/supplementary material/referenced in article.

Declaration of interests statement

The authors declare no conflict of interest.

Additional information

No additional information is available for this paper.

Acknowledgements

The authors (LAK and KRSP) would like to thank the Management and Trust of Koneru Lakshmaiah Education Foundation Vaddeswaram, Andhra Pradesh, India, for providing the necessary laboratory facilities to carry out research work. The authors also thank the Centre for Advanced Material Technology, Ramaiah Institute of Technology, Bangalore for TG and DSC analysis.

References

[1] C. Contado, Nanomaterials in consumer products: a challenging analytical problem, Front. Chem. 3 (2015) 48.
[2] Q. Qiu Zhao, A. Boxman, U. Chowdhry, Nanotechnology in the chemical industry – opportunities and challenges, J. Nanoparticle Res. 5 (2003) 567–572.
[3] L. Xu, C. Srinivasakannan, J. Peng, L. Zhang, D. Zhang, Synthesis of Cu-CuO nanocomposite in microreactor and its application to photocatalytic degradation, J. Alloys Compd. 695 (2017) 263–269.
[4] J. Pal, M. Ganguly, S. Dutta, C. Mondal, Y. Negishi, T. Pal, Hierarchical Au–CuO nanocomposite from redox transformation reaction for surface enhanced Raman scattering and clock reaction, CrystEngComm 16 (2014) 883–893.
[5] S. Stankic, S. Suman, F. Haque, J. Vidic, Pure and multi metal oxide nanoparticles: synthesis, antibacterial and cytotoxic properties, J. Nanobiotechnol. 14 (2016) 73.
[6] R. Khan, R. Ahmad, P. Rai, L.-W. Jang, J.-H. Yun, Y.-T. Yu, Y.-B. Hahn, I.-H. Lee, Glucose-assisted synthesis of Cu_2O shuriken-like nanostructures and their application as nonenzymatic glucose biosensors, Sensor. Actuator. B Chem. 203 (2014) 471–476.
[7] J.-L. Cao, G.-S. Shao, Y. Wang, Y. Liu, Z.-Y. Yuan, CuO catalysts supported on attapulgite clay for low-temperature CO oxidation, Catal. Commun. 9 (2008) 2555–2559.
[8] C.-Y. Chiang, K. Aroh, N. Franson, V.R. Satsangi, S. Dass, S. Ehrman, Copper oxide nanoparticle made by flame spray pyrolysis for photoelectrochemical water splitting – Part II. Photoelectrochemical study, Int. J. Hydrogen Energy 36 (2011) 15519–15526.
[9] Y. Wang, Q.-W. Yang, Q. Yang, T. Zhou, M.-F. Shi, C.-X. Sun, X.-X. Gao, Y.-Q. Cheng, X.-G. Cui, Y.-H. Sun, Cuprous oxide nanoparticles inhibit prostate cancer by attenuating the stemness of cancer cells via inhibition of the Wnt signalling pathway, Int. J. Nanomed. 12 (2017) 2569–2579.
[10] P. Subalakshmi, A. Sivashanmugam, CuO nano hexagons, an efficient energy storage material for Li-ion battery application, J. Alloys Compd. 690 (2017) 523–531.
[11] G. Varughese, V. Rini, S.P. Suraj, K.T. Usha, Characterisation and optical studies of copper oxide nanostructures doped with lanthanum ions, Adv. Mater. Sci. 14 (2014) 49–60.
[12] K. Giannousi, E. Hatzivassiliou, S. Mourdikoudis, G. Vourlias, A. Pantazaki, C. Dendrinou-Samara, Synthesis and biological evaluation of PEGylated CuO nanoparticles, J. Inorg. Biochem. 164 (2016) 82–90.
[13] G. Borkow, J. Gabbay, A. Lyakhovitsky, M. Huszar, Improvement of facial skin characteristics using copper oxide containing pillowcases: a double-blind, placebo-controlled, parallel, randomized study, Int. J. Cosmet. Sci. 31 (2009) 437–443.
[14] G. Borkow, R.C. Zatcoff, J. Gabbay, Reducing the risk of skin pathologies in diabetics by using copper impregnated socks, Med. Hypotheses 73 (2009) 883–886.
[15] K. Velsankar, S. Suganya, P. Muthumari, S. Mohandoss, S. Sudhahar, Ecofriendly green synthesis, characterization and biomedical applications of CuO nanoparticles synthesized using leaf extract of Capsicum frutescens, J. Environ. Chem. Eng. 9 (2021) 106299.
[16] S. Logambal, C. Maheswari, S. Chandrasekar, T. Thilagavathi, C. Inmozhi, S. Panimalar, F.A. Bassyouni, et al., Synthesis and characterizations of CuO nanoparticles using couroupita guianensis extract for and antimicrobial applications, J. King Saud Univ. Sci. 34 (2022) 101910.
[17] I.H. Shah, M. Ashraf, I.A. Sabir, M.A. Manzoor, et al., Green synthesis and Characterization of Copper oxide nanoparticles using Calotropis procera leaf extract and their different biological potentials, J. Mol. Struct. (2022) 132696.
[18] P.G. Bhavyasree, T.S. Xavier, Green synthesised copper and copper oxide-based nanomaterials using plant extracts and their application in antimicrobial activity: Review, Curr. Res. Green Sustain. Chem. 5 (2022) 100249.
[19] N. Najafianpour, D. Dorranian, Properties of graphene/Au nanocomposite prepared by laser irradiation of the mixture of individual colloids, Appl. Phys. A. 124 (2018) 805.
[20] S. Barua, G. Das, L. Aidew, A.K. Buragohain, N. Karak, Copper–copper oxide coated nanofibrillar cellulose: a promising biomaterial, RSC Adv. 3 (2013) 14997.
[21] D. Letchumanan, S.P.M. Sok, S. Ibrahim, N.H. Nagoor, N.M. Arshad, Plant-based biosynthesis of copper/copper oxide nanoparticles: an update on their applications in biomedicine, mechanisms, and toxicity, Biomolecules 11 (2021) 564.
[22] B. Jia, Y. Mei, L. Cheng, J. Zhou, L. Zhang, Preparation of copper nanoparticles coated cellulose films with antibacterial properties through one-step reduction, ACS Appl. Mater. Interfaces 4 (2012) 2897–2902.
[23] M. Bost, S. Houdart, M. Oberli, E. Kalonji, J.-F. Huneau, I. Margaritis, Dietary copper and human health: current evidence and unresolved issues, J. Trace Elem. Med. Biol. 35 (2016) 107–115.
[24] V.D. Mendhulkar, A. Yadav, Anticancer activity of camellia sinensis mediated copper nanoparticles against HT-29, MCF-7 and MOLT-4 human cancer cell lines, Asian J. Pharmaceut. Clin. Res. 10 (2017) 82.
[25] C. Santini, M. Pellei, V. Gandin, M. Porchia, F. Tisato, C. Marzano, Advances in copper complexes as anticancer agents, Chem. Rev. 114 (2014) 815–862.
[26] Q. Maqbool, S. Iftikhar, M. Nazar, F. Abbas, A. Saleem, T. Hussain, R. Kausar, S. Anwaar, N. Jabeen, Green fabricated CuO nanobullets via *Olea europaea* leaf extract shows auspicious antimicrobial potential, IET Nanobiotechnol. 11 (2017) 463–466.
[27] R.M.S.A.-H. Wisam, M. Mohammed, Tahseen H. Mubark, Effect of CuO nanoparticles on antimicrobial activity prepared by sol-gel method, Int. J. Appl. Eng. Res. 13 (2018) 10559–10562.

[28] A. Jurj, C. Braicu, L.-A. Pop, C. Tomuleasa, C. Gherman, I. Berindan-Neagoe, The new era of nanotechnology, an alternative to change cancer treatment, Drug Des. Dev. Ther. 11 (2017) 2871–2890.

[29] L. Castillo-Henríquez, K. Alfaro-Aguilar, J. Ugalde-Álvarez, L. Vega-Fernández, G. Montes de Oca-Vásquez, J.R. Vega-Baudrit, Green synthesis of gold and silver nanoparticles from plant extracts and their possible applications as antimicrobial agents in the agricultural area, Nanomaterials 10 (2020) 1763.

[30] H. Mersian, M. Alizadeh, Effect of diverse Pechini sol-gel parameters on the size, morphology, structural and optical properties of the Tenorite (CuO) NPs: a facile approach for desired properties, Ceram. Int. 46 (2020) 17197–17208.

[31] S.A. Ayon, M.M. Billah, S.S. Nishat, A. Kabir, Enhanced photocatalytic activity of Ho^{3+} doped ZnO NPs synthesized by modified sol-gel method: an experimental and theoretical investigation, J. Alloys Compd. 856 (2021) 158217.

[32] R. Zamiri, B.Z. Azmi, M. Darroudi, A.R. Sadrolhosseini, M.S. Husin, A.W. Zaidan, M.A. Mahdi, Preparation of starch stabilized silver nanoparticles with spatial self-phase modulation properties by laser ablation technique, Appl. Phys. A. 102 (2011) 189–194.

[33] M. Darroudi, M.B. Ahmad, R. Zamiri, A.H. Abdullah, N.A. Ibrahim, A.R. Sadrolhosseini, Time-dependent preparation of gelatin-stabilized silver nanoparticles by pulsed Nd: YAG laser, Solid State Sci. 13 (2011) 520–524.

[34] Z. Sabouri, A. Akbari, H.A. Hosseini, M. Khatami, M. Darroudi, Egg white-mediated green synthesis of NiO nanoparticles and study of their cytotoxicity and photocatalytic activity, Polyhedron 178 (2020) 114351.

[35] A.M. El Shafey, Green synthesis of metal and metal oxide nanoparticles from plant leaf extracts and their applications: a review, Green Process. Synth. 9 (2020) 304–339.

[36] Z. Sabouri, M. Sabouri, M.S. Amiri, M. Khatami, M. Darroudi, Plant-based synthesis of cerium oxide nanoparticles using *Rheum turkestanicum* extract and evaluation of their cytotoxicity and photocatalytic properties, Mater. Technol. (2020) 1–14.

[37] M.S.A. Miri, N. Dorani, M. Darroudi, Green synthesis of silver nanoparticles using *Salvadora persica* L. and its antibacterial activity, Cell. Mol. Biol. 62 (2016) 46–50.

[38] J.B. Harborne, Indian medicinal plants. A compendium of 500 species, in: P.K. Warrier, V.P.K. Nambiar, C. Ramankutty (Eds.), J. Pharm. Pharmacol. 46 (2011) 935. Vol.1.

[39] K. Zahara, S. Tabassum, S. Sabir, M. Arshad, R. Qureshi, M.S. Amjad, S.K. Chaudhari, A review of therapeutic potential of *Saussurea lappa*-An endangered plant from Himalaya, Asian Pac. J. Trop. Med. 7 (2014) S60–S69.

[40] Vijay Veer, R. Gopalakrishnan (Eds.), Herbal Insecticides, Repellents and Biomedicines: Effectiveness and Commercialization, Springer India, New Delhi, 2016.

[41] J.H. Jung, Y. Kim, C.-O. Lee, S.S. Kang, J.-H. Park, K.S. Im, Cytotoxic constituents of Saussurea lappa, Arch Pharm. Res. (Seoul) 21 (1998) 153–156.

[42] G. Singhal, R. Bhavesh, K. Kasariya, A.R. Sharma, R.P. Singh, Biosynthesis of silver nanoparticles using *Ocimum sanctum* (Tulsi) leaf extract and screening its antimicrobial activity, J. Nanoparticle Res. 13 (2011) 2981–2988.

[43] N. Ahmad, M.K. Alam, V.N. Singh, S.F. Shamsi, S. Sharma, Ocimum mediated biosynthesis of silver nanoparticles, in: 2009 Fifth Int. Conf. MEMS NANO, Smart Syst., IEEE, 2009, pp. 80–84.

[44] G. Singhal, R. Bhavesh, A.R. Sharma, R.P. Singh, Ecofriendly biosynthesis of gold nanoparticles using medicinally important *Ocimum basilicum* leaf extract, Adv. Sci. Eng. Med. 4 (2012) 62–66.

[45] C. Soundarrajan, A. Sankari, P. Dhandapani, S. Maruthamuthu, S. Ravichandran, G. Sozhan, N. Palaniswamy, Rapid biological synthesis of platinum nanoparticles using *Ocimum sanctum* for water electrolysis applications, Bioproc. Biosyst. Eng. 35 (2012) 827–833.

[46] K.S. Shivani Dagar, Ishika Shah, Kirti Kumari, Kiran Pal, Gita Batra Narula, Kiran Soni, Green synthesis of copper nanoparticles designed from *Ocimum sanctum* for purification of waste water, Vantage J. Themat. Anal. 1 (1) (2020) 32–40.

[47] H. Abdul Salam, R. Sivaraj, R. Venckatesh, Green synthesis and characterization of zinc oxide nanoparticles from *Ocimum basilicum* L. var. purpurascens Benth.-Lamiaceae leaf extract, Mater. Lett. 131 (2014) 16–18.

[48] S. Batakurki, J. Kumar Ashwini, Biogenic synthesis, antibacterial and antioxidant studies of prepared silver nano particles using root extract of *Saussurea lappa*, Int. J. New Technol. Sci. Eng. 6 (2019) 11–21.

[49] M. Amina, N.M. Al Musayeib, N.A. Alarfaj, M.F. El-Tohamy, H.F. Oraby, G.A. Al Hamoud, S.I. Bukhari, N.M.S. Moubayed, Biogenic green synthesis of MgO nanoparticles using *Saussurea costus* biomasses for a comprehensive detection of their antimicrobial, cytotoxicity against MCF-7 breast cancer cells and photocatalysis potentials, PLoS One 15 (2020), e0237567.

[50] M.S. Al-Saggaf, A.A. Tayel, M.O.I. Ghobashy, M.A. Alotaibi, M.A. Alghuthaymi, S.H. Moussa, Phytosynthesis of selenium nanoparticles using the *costus* extract for bactericidal application against foodborne pathogens, Green Process. Synth. 9 (2020) 477–487.

[51] L.A. Kolahalam, K.R.S. Prasad, P. Murali Krishna, N. Supraja, *Saussurea lappa* plant rhizome extract-based zinc oxide nanoparticles: synthesis, characterization and its antibacterial, antifungal activities and cytotoxic studies against Chinese Hamster Ovary (CHO) cell lines, Heliyon 7 (2021), e07265.

[52] Y. Xue, G. Yu, Z. Shan, Z. Li, Phyto-mediated synthesized multifunctional Zn/CuO NPs hybrid nanoparticles for enhanced activity for kidney cancer therapy: a complete physical and biological analysis, J. Photochem. Photobiol. B Biol. 186 (2018) 131–136.

[53] S.J. Hoseini, M. Darroudi, R. Kazemi Oskuee, L. Gholami, A. Khorsand Zak, Honey-based synthesis of ZnO nanopowders and their cytotoxicity effects, Adv. Powder Technol. 26 (2015) 991–996.

[54] J. Van Meerloo, G.J.L. Kaspers, J. Cloos, Cell sensitivity assays: the MTT assay, Methods Mol. Biol. 731 (2011) 237–245.

[55] J. Liu, X. Huang, Y. Li, K.M. Sulieman, X. He, F. Sun, Hierarchical nanostructures of cupric oxide on a copper substrate: controllable morphology and wettability, J. Mater. Chem. 16 (2006) 4427.

[56] A. Kumar, C.K. Dixit, Methods for characterization of nanoparticles, in: Adv. Nanomedicine Deliv. Ther. Nucleic Acids, Elsevier, 2017.

[57] A. Tadjarodi, R. Roshani, A green synthesis of copper oxide nanoparticles by mechanochemical method, Curr. Chem. Lett. 3 (2014) 215–220.

[58] A.R. Saeid Taghavi Fardood, Green synthesis and characterization of copper oxide nanoparticles using coffee powder extract, J. Nanostructures. 6 (2016) 167–171.

[59] Z. Sabouri, A. Akbari, H.A. Hosseini, A. Hashemzadeh, M. Darroudi, Bio-based synthesized NiO nanoparticles and evaluation of their cellular toxicity and wastewater treatment effects, J. Mol. Struct. 1191 (2019) 101–109.

[60] Z. Sabouri, A. Akbari, H.A. Hosseini, A. Hashemzadeh, M. Darroudi, Eco-friendly biosynthesis of nickel oxide nanoparticles mediated by *okra* plant extract and investigation of their photocatalytic, magnetic, cytotoxicity, and antibacterial properties, J. Clust. Sci. 30 (2019) 1425–1434.

[61] M. Nasrollahzadeh, M. Atarod, S.M. Sajadi, Green synthesis of the Cu/Fe_3O_4 nanoparticles using Morinda morindoides leaf aqueous extract: a highly efficient magnetically separable catalyst for the reduction of organic dyes in aqueous medium at room temperature, Appl. Surf. Sci. 364 (2016) 636–644.

[62] K.R. Raghupathi, R.T. Koodali, A.C. Manna, Size-Dependent bacterial growth inhibition and mechanism of antibacterial activity of zinc oxide nanoparticles, Langmuir 27 (2011) 4020–4028.

[63] Zarrindokht Emami-Karvani, Antibacterial activity of ZnO nanoparticle on Gram-positive and Gram-negative bacteria, Afr. J. Microbiol. Res. 5 (2011) 1368–1373.

[64] K.M. Reddy, K. Feris, J. Bell, D.G. Wingett, C. Hanley, A. Punnoose, Selective toxicity of zinc oxide nanoparticles to prokaryotic and eukaryotic systems, Appl. Phys. Lett. 90 (2007) 213902.

[65] A. Edreva, Generation and scavenging of reactive oxygen species in chloroplasts: a submolecular approach, Agric. Ecosyst. Environ. 106 (2005) 119–133.

[66] Q.L. Feng, J. Wu, G.Q. Chen, F.Z. Cui, T.N. Kim, J.O. Kim, A mechanistic study of the antibacterial effect of silver ions on *Escherichia coli* and *Staphylococcus aureus*, J. Biomed. Mater. Res. 52 (2000) 662–668.

[67] I.P. Mukha, A.M. Eremenko, N.P. Smirnova, A.I. Mikhienkova, G.I. Korchak, V.F. Gorchev, A.Y. Chunikhin, Antimicrobial activity of stable silver nanoparticles of a certain size, Appl. Biochem. Microbiol. 49 (2013) 199–206.

[68] S. Behzadi, V. Serpooshan, W. Tao, M.A. Hamaly, M.Y. Alkawareek, E.C. Dreaden, D. Brown, A.M. Alkilany, O.C. Farokhzad, M. Mahmoudi, Cellular uptake of nanoparticles: journey inside the cell, Chem. Soc. Rev. 46 (2017) 4218–4244.

[69] A. Ivask, A. ElBadawy, C. Kaweeteerawat, D. Boren, H. Fischer, Z. Ji, C.H. Chang, R. Liu, T. Tolaymat, D. Telesca, J.I. Zink, Y. Cohen, P.A. Holden, H.A. Godwin, Toxicity mechanisms in *Escherichia coli* vary for silver nanoparticles and differ from ionic silver, ACS Nano 8 (2014) 374–386.